

Hydroelastic response of a floating runway to cnoidal waves

R. C. Ertekin^{1,a)} and Dingwu Xia²

¹*Department of Ocean and Resources Engineering, University of Hawaii at Manoa, Honolulu, Hawaii 96822, USA*

²*Engineering Services, British Petroleum GoM, Houston, Texas 77079, USA*

(Received 20 June 2013; accepted 19 December 2013; published online 5 February 2014)

The hydroelastic response of mat-type Very Large Floating Structures (VLFSs) to severe sea conditions, such as tsunamis and hurricanes, must be assessed for safety and survivability. An efficient and robust nonlinear hydroelastic model is required to predict accurately the motion of and the dynamic loads on a VLFS due to such large waves. We develop a nonlinear theory to predict the hydroelastic response of a VLFS in the presence of cnoidal waves and compare the predictions with the linear theory that is also developed here. This hydroelastic problem is formulated by directly coupling the structure with the fluid, by use of the Level I Green-Naghdi theory for the fluid motion and the Kirchhoff thin plate theory for the runway. The coupled fluid structure system, together with the appropriate jump conditions are solved in two-dimensions by the finite-difference method. The numerical model is used to study the nonlinear response of a VLFS to storm waves which are modeled by use of the cnoidal-wave theory. Parametric studies show that the nonlinearity of the waves is very important in accurately predicting the dynamic bending moment and wave run-up on a VLFS in high seas. © 2014 AIP Publishing LLC. [<http://dx.doi.org/10.1063/1.4862916>]

I. INTRODUCTION

The research and development of mat-type Very Large Floating Structures (VLFSs) has made significant progress since the First International Workshop on Very Large Floating Structures (VLFS'91) was held in Hawaii in April 1991 when the acronym "VLFS" was first coined by Ertekin and Riggs.¹ Watanabe *et al.*² provide a list of conference proceedings and journal issues dedicated to the VLFSs, and a review of recent research progress on the hydroelasticity of mat-type VLFS, and it complements a previous survey on the prediction of hydroelastic responses of VLFS by Kashiwagi.³ The overview by Ohmatsu⁴ is more related to the Mega-float project.

The size of a VLFS presents a significant challenge to engineers and researchers since it is difficult to scale simultaneously the structural and hydrodynamic properties of a VLFS model in a wave tank, and the existing hydroelasticity theories such as by Wu⁵ are not necessarily efficient enough especially for preliminary design purposes. Therefore, most of the recent research during the last two decades has focused on developing efficient numerical tools by simplifying the structural model.

Among the numerous numerical methods on the hydroelasticity of a VLFS, most of them are within the scope of linear wave theory and in frequency domain or time domain. There are only a few numerical models that consider the global hydroelastic response of a VLFS to nonlinear waves, which is a naturally complicated phenomenon.

In linear hydroelasticity analysis of a mat-type VLFS, the flow is usually assumed to be governed by linear potential theory. The wave amplitude is therefore assumed to be infinitesimal so that the

^{a)} Author to whom correspondence should be addressed. Electronic mail: ertekin@hawaii.edu.

nonlinearities can be ignored. A VLFS is generally modeled as an elastic thin plate and only the vertical motion is considered. It is also assumed that there is no gap between the VLFS and the free surface, i.e., no slamming is allowed.

More often, the hydroelastic analysis is carried out in the frequency domain since this is more straightforward than it would have been in the time domain. The fluid problem is generally solved by the boundary-integral method, i.e., by use of the Green function. The plate response is often solved by the Finite Element Method (FEM), or alternatively, as part of the boundary-element of the fluid domain.

There have been two major approaches to the frequency-domain analysis: the modal expansion method and the direct method. Modified modal functions have been introduced by many authors, primarily to increase the numerical efficiency of the computations. The products of free-free beam modes (Wu *et al.*⁶ and Nagata *et al.*⁷), the B-spline function (Kashiwagi⁸), and two-dimensional polynomial functions (Wang *et al.*⁹) are some examples. The direct method solves the equation of motion of the plate and the hydrodynamic problem simultaneously using the pressure distribution method, as pioneered by Mamidipudi and Webster.¹⁰ Ma¹¹ introduced a high-order method using a double fifth-order interpolation function to improve the computational efficiency in an effort to optimize the stiffness of the floating runway. Kashiwagi¹² proposed the B-spline function for both pressure and plate deformation to reduce the computational time. Another direct method developed by Ohkusu and Namba¹³ considers the mat-type VLFS as part of the water surface with different physical properties represented by a Green function.

Based on the shallow-water, linear Green-Naghdi theory, Ertekin and Kim¹⁴ developed another direct method by dividing the fluid domain into areas with and without the plate and matching them on the juncture boundary by use of the continuity of mass flux and mean pressure. Benchmark tests conducted by Riggs *et al.*¹⁵ show good agreement between the linear GN results and the solutions obtained from other three-dimensional hydroelastic models based on potential theories (e.g., HYDRAN¹⁶ and Iijima *et al.*¹⁷) over a wide range of wave periods. This method was used in the analysis of the effects of a shoreline and a breakwater on a floating runway with high efficiency, as shown by Xia *et al.*¹⁸ and Ertekin *et al.*¹⁹

Only a few studies of transient problems have been reported to date, and most of them are still too computationally intensive for practical use in VLFS design. The commonly used approaches for time-domain analysis of VLFS can be categorized as the direct integration method and the Fourier transform method. It is well-known that the time-domain and frequency domain analysis is reversible through Fourier transformation. Ohmatsu²⁰ and Miao *et al.*²¹ transferred the frequency-domain response for the fluid domain into the time-domain with the Fourier transform, and solved the plate transient response due to irregular waves, impact or moving loads (i.e., idealized airplane landing or take-off), and nonlinear mooring-load cases. However, the truncation of the higher modes may cut off contributions from higher frequencies as pointed out by Kashiwagi.³

The nonlinear hydroelastic analysis under large waves, such as during a hurricane, typically must be done in the time-domain, using a direct integration method. Other nonlinear hydroelastic phenomena such as slamming (Faltinsen²²) and the steady drift force (e.g., Kim and Ertekin²³ and Kashiwagi²⁴) may also be important in VLFS design, but are not discussed here.

Liu and Sakai²⁵ developed a two-dimensional nonlinear model to simulate the hydroelastic response of an elastic beam to random waves, and nonperiodic nonlinear waves such as a tsunami. In their study, the boundary-element method (BEM) is used for the fluid domain that is based the Rankine source method, and the structural deformation of the beam is calculated by the finite-element method. The fluid motion and structure are coupled by satisfying the continuity of the pressure and displacement on the fluid-structure interface. The computational efficiency for the Rankine-source-based BEM somehow limits the application of this numerical model to VLFS analysis with the present CPU technology although it is accurate and versatile in its application.

Takagi^{26,27} studied the response of a mat-type VLFS to a tsunami in two-dimensions and three-dimensions, respectively. A nonlinear shallow-water wave equation, i.e., the generalized Boussinesq equation (Wu²⁸) was used for the fluid motion. The shallow-water wave theory is very efficient since the unknowns are only functions of the spatial coordinates on the horizontal plane and time. Thin plate theory was used for the plate motion with the acceleration term ignored. The matched

asymptotic expansion method was used to connect the outer solution governed by the Boussinesq equations and the inner solution governed by the Laplace equation. It was shown that higher-order terms play an important role in the prediction of VLFS response to nonlinear tsunami waves. It is noted that small oscillations occur in the surface elevation snapshots taken at the free surface close to the edge of the plate (see Figure 3 of Takagi²⁶). This may be introduced by the matching scheme which may not ensure that the conservation laws are satisfied at the matching interface.

Recently, Xia *et al.*²⁹ proposed a new 2D nonlinear model to calculate the hydroelastic response of mat-type VLFSs to solitary waves, based on the Level I Green-Naghdi (GN) equations (Green and Naghdi³⁰). The VLFS is represented by an elastic plate. A new set of jump conditions are derived to match the fluid solutions at both sides of the plate edge through the use of the postulated conservation laws of mass, momentum, and mechanical energy. We anticipate that this numerical model has a similar computational efficiency to that of Takagi²⁶ with an improved matching condition. The noise at the vicinity of the plate edge in Takagi²⁶ does not appear in results of Xia *et al.*²⁹

In this work, a two-dimensional nonlinear hydroelasticity model is developed. The nonlinear wave problem is governed by the Level I Green-Naghdi theory (see, e.g., Green and Naghdi³⁰), and the mat-type VLFS is simplified as an elastic plate which is modeled using the Kirchhoff thin plate theory (see, e.g., Timoshenko and Woinowsky-Krieger³¹). It is assumed that no gap exists between the VLFS bottom and water surface so that the structural and fluid motion can be coupled by use of the continuity of both pressure and displacement at the interface. At the plate edges, a set of jump conditions suitable for the current three-dimensional nonlinear hydroelasticity analysis is developed based on the integral balance laws. These conditions ensure that the solution satisfies the conservation of mass, momentum, and energy through the jump interface. The nonlinear Level I GN theory is numerically modeled to determine the hydroelastic response of a mat-type VLFS to waves with unsteady jump conditions very efficiently (see, e.g., Ertekin and Kim¹⁴ and Xia *et al.*²⁹). The proper boundary and initial conditions are derived to make the formulation complete. With the help of the mass continuity equation, the system of equations is simplified further by removing the terms that are time derivatives of the surface elevation from the momentum equations, following Ertekin *et al.*³²

The three-dimensional model is then simplified to two dimensions so that the basics of the nonlinear hydroelasticity can be more clearly examined with a simpler system. The nonlinear model is also linearized to study the dispersion relation of the hydroelastic wave and to observe the nonlinear effects.

Finite Difference Method (FDM), with the 4th-order Runge-Kutta method for time stepping, and a central difference for the spatial variables, is used to solve the partial differential equation system. The numerical method is then used to study the response of a VLFS to large design waves where the storm waves are modeled by cnoidal waves.

In the present work, we first introduce the nonlinear theory and then linearize the governing equations of the problem to obtain the linear solution of the same problem. Following this, the finite-difference method is introduced and the solution approach is detailed. Finally, we present the results for both the linear and cnoidal wave solutions of the problem and emphasize the importance of nonlinearity in the structural response of a floating runway.

II. THEORY

The coordinate system and geometry of the fluid-structure system of the two-dimensional problem are shown in Fig. 1. The beam is taken from a strip of unit width from a plate of large aspect ratio (beam length over beam width ratio is large). The beam is envisioned as the strip of a floating runway that freely floats on the top of Region II, with a draft d , length b , and thickness h_p . In Fig. 1, m is the mass per unit length of the beam (that is of unit width). Its thickness is much smaller than its length so that the Kirchhoff thin-plate theory can be applied. The wave propagates parallel to the beam-length direction so that the hydroelastic phenomenon also is two dimensional.

The whole domain is divided into three parts. Regions I and III contain the ordinary shallow-water wave problems. Nonlinear cnoidal waves propagate from left to right and excite the motion of

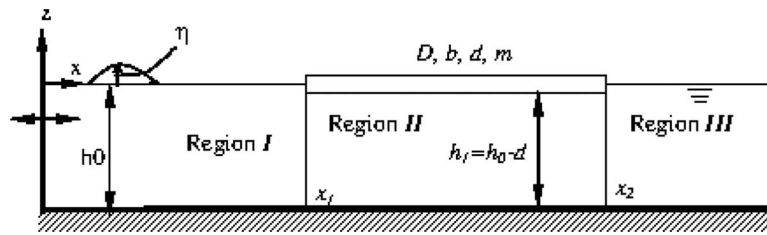


FIG. 1. Definition sketch of the problem.

the beam. The inviscid fluid motion is assumed to be governed by the Level I GN theory (see, e.g., Ertekin and Wehausen³³). The sea floor is flat. The still-water depth in the open water area is h_0 , and in Region II, it is $h_0 - d$. We further assume that the runway is horizontally restrained somehow, perhaps with mooring dolphins, and thus, no horizontal motion in the x direction is allowed.

A. Nonlinear theory

The governing equations for the motion of the fluid are provided by the Level I Green-Naghdi (GN) theory (see, e.g., Green and Naghdi³⁰). They can be written in a compact form (see, e.g., Ertekin and Becker³⁴):

$$\eta_t + \frac{\partial [(h + \eta)u]}{\partial x} = 0, \quad (1)$$

$$\dot{u} + g\eta_x + \frac{\hat{p}_x}{\rho} = -\frac{1}{6} [4\eta_x \ddot{\eta} + 2(h + \eta)(\ddot{\eta})_x], \quad (2)$$

where, ρ is the mass density of water, \hat{p} is the pressure on the upper surface of the water column, and η is the surface displacement, and $u(x, t)$ is the horizontal velocity of fluid particles in the x direction. The subscripts, x and t , denote the partial derivatives, g is the gravitational acceleration, h the still-water depth, and equals to h_0 in Regions I and III, and to h_1 in Region II. The superposed dot denotes the material derivative, i.e., $\dot{\eta} = \eta_t + u \partial \eta / \partial x$. When there is no plate floating on the top of the fluid surface, the atmospheric pressure, \hat{p} , is set to zero. In Region II, however, \hat{p} equals to the pressure on the bottom of the plate, while the atmospheric pressure on the top of the plate is set to zero.

It is noted that the integrated pressure through the water column, in the Level I GN theory, is given by (see, e.g., Ertekin³⁵)

$$P = \frac{1}{6} \rho (h + \eta)^2 (2\ddot{\eta} + 3g) + \hat{p}(h + \eta). \quad (3)$$

Since we are considering long waves, the linear beam theory (one-dimensional version of the linear thin plate theory) is applied to the structure, i.e.,

$$m\eta_{tt} + D\eta_{xxxx} + mg = \hat{f}, \quad (4)$$

where \hat{f} is the force acting by water on the bottom of plate, i.e., \hat{p} times the width of the beam, D is the flexural rigidity of the plate, and is defined by $D = Eh_p^3 / [12(1 - \nu^2)]$, and E and ν are Young's modulus and Poisson's ratio of the plate, respectively. It is noted that the dimension of each term in Eq. (4) is force/length since we are considering a beam of unit width.

The motion of the fluid and the plate is coupled through the dynamic free-surface condition. We also assume that the displacement of the plate and the fluid-surface elevation under the bottom of the plate are the same, i.e., no air gap is allowed. After we substitute \hat{f} from Eq. (4) into Eq. (2), and use the fact that the continuity equation is the same as in Eq. (1), except for the fluid

sheet thickness, we can obtain the governing equations for the fluid-plate Region II:

$$\eta_t + \frac{\partial [(h_1 + \eta)u]}{\partial x} = 0, \quad (5)$$

$$\dot{u} + g\eta_x + \frac{(m\eta_{tt} + D\eta_{xxxx} + mg)_x}{\rho} = -\frac{1}{6} [4\eta_x\ddot{\eta} + 2(h_1 + \eta)(\ddot{\eta})_x]. \quad (6)$$

The Eqs. (5) and (6) are the modified Level I GN equations (2D) that are nonlinear.

It is very desirable to remove the time dependent terms in the combined momentum equation, Eq. (6), in numerically solving the set of modified GN equations. This was done by Xia,³⁶ and as a result Eq. (6) becomes

$$(1 - m\eta_{xx})u_t - [\eta_x(h_1 + \eta) + 2m\eta_x]u_{xt} - \left[\frac{1}{3}(h_1 + \eta)^2 + m(h_1 + \eta)\right]u_{xxt} = -Y_f - Y_p, \quad (7)$$

where

$$Y_f = \eta_x(h_1 + \eta)(u_x^2 - uu_{xx}) + \frac{1}{3}(h_1 + \eta)^2(u_x u_{xx} - uu_{xxx}) + uu_x + \eta_x, \quad (8)$$

$$Y_p = m[(h_1 + \eta)(3u_x u_{xx} + uu_{xxx}) + D\eta_{xxxxx} + \eta_{xxx}u^2 + 5\eta_{xx}uu_x + 4\eta_x(u_x^2 + uu_{xx})] - \hat{p}ld. \quad (9)$$

1. Initial and boundary conditions

We assume that there are waves initially ($t = 0$) and they are at a distance away from the plate. The velocities and surface elevation are initially set according to the analytical solution of a cnoidal wave that the Level I GN theory provides (see, e.g., Sun³⁷ and Ertekin and Becker³⁴):

$$\eta_0(t) = \eta_2 + H\mathbf{Cn}^2, \quad u_0(t) = \frac{c\eta_0}{1 + \eta_0}, \quad c = \sqrt{(1 + \eta_1)(1 + \eta_2)(1 + \eta_3)}, \quad (10)$$

where \mathbf{Cn} is the Jacobian elliptic cosine function, H is the wave height, c is the phase speed, and

$$\eta_1 = \frac{-H}{k^2} \frac{E}{K}, \quad \eta_2 = \frac{H}{k^2} \left(1 - k^2 - \frac{E}{K}\right), \quad \eta_3 = \eta_2 + H, \quad k^2 = \frac{H}{\eta_3 - \eta_1}, \quad (11)$$

and K and E are the complete elliptic integrals of the first and second kind, respectively. The dispersion relation is given by

$$\lambda = ckK\sqrt{\frac{16}{3H}}, \quad (12)$$

where λ is the wavelength. Clearly, the wave period is given by

$$T_{cn} = kK\sqrt{\frac{16}{3H}}. \quad (13)$$

To prevent the cnoidal waves to apply a sudden pressure force on the domain that may lead to instabilities, the wave is modulated in the front by a ramp function also used by e.g., Ertekin and Becker.³⁴ The piston wave-maker generates waves by having its velocity specified such that the generated waves are consistent with the initial wave inside the domain. The downwave boundary is an open boundary. The open boundary condition used there is the Orlandi condition, and it was used before successfully (see, e.g., Ertekin *et al.*³²).

At the ends of the plate, free-free end boundary conditions of the beam require the vanishing of the bending moment and shear force. Thus, we have

$$D\eta_{xx} = D\eta_{xxx} = 0 \text{ at } x = x_1^+ \text{ and } x_2^-. \quad (14)$$

Since we assume that there is no gap between the bottom surface of the beam and the top surface of the fluid layer, the fluid under the tip of the beam should also satisfy the conditions given by

Eq. (14). Because $\eta_{xx}|_{x_i} = 0$ and $\eta_{xxx}|_{x_i} = 0$ ($i = 1, 2$) at any time t , $\eta_{xxt}|_{x_i} = 0$ and $\eta_{xxx}|_{x_i} = 0$ should be satisfied for all t . By taking the second and third derivatives about x on both sides of the mass continuity equation, Eq. (5), we obtain the boundary conditions for the fluid motion under the ends of the beam as (at $x = x_i$, $i = 1, 2$)

$$3\eta_x u_{xx} + (h + \eta)u_{xxx} = 0, \quad (15)$$

$$4\eta_x u_{xxx} + (h + \eta)u_{xxxx} + \eta_{xxx}u = 0. \quad (16)$$

2. Jump conditions

In the following formulation, only the left side of the elastic plate is treated here because the solution for the other side is obtained by employing the same technique. The appropriate jump conditions are demanded by the theory because the fluid surface is discontinuous at the juncture of Regions *I* and *II*, $x = x_1^\pm$ when the fluid is quiescent as the water depths are different to the left and right of the discontinuity. Here, “+” denotes the limit approaching from right toward x_1 , while “-” from left toward x_1 . The jump conditions are necessary for having the mass and momentum (and thus mechanical energy in the absence of any heat flux) at $x = x_1^\pm$ conserved.

Naghdi and Rubin³⁸ provided a set of jump conditions for a flat bottom and steady motion by use of the conservation laws and when there is a rigid body floating on the fluid surface. Naghdi and Rubin,³⁸ and also Green and Naghdi,³⁹ applied them to a steady-flow problem. However, they additionally required the continuity of the surface elevation and surface pressure, \hat{p} , or the slope of the surface. In the present study, however, we cannot avoid discontinuities in the surface elevation and pressure since the motion of the elastic beam is relative at $x = x_1^-$ and x_1^+ .

Based on the conservation of mass, momentum, director momentum (moment of vertical momentum), and mechanical energy (Naghdi and Rubin³⁸), the jump conditions for the case of a floating, elastic body can be derived and specialized to the unsteady problem under consideration here. We assume the singularity to be stationary in the horizontal plane and identify the fixed location of the discontinuity by the vertical line at $x = x_1$. The sea bed is also assumed to be stationary in the present derivation, although this is not necessary in general. By use of Leibnitz’s rule, and by following Naghdi and Rubin,³⁸ the corresponding jump conditions for mass, horizontal and vertical momentum, director momentum, and energy conservation can be derived. An alternative derivation was given by Xia³⁶ and Xia *et al.*²⁹

The two-dimensional jump conditions in the format of reduced order of the time derivatives at the left end of the beam, $x = x_l$, are presented as

$$[(h_0 + \eta)u] |_{x_l^-} = [(h_1 + \eta)u] |_{x_l^+}, \quad (17)$$

$$[-S_0 u_{xt} + Y_0] |_{x_l^-} = [R_1 u_t - S_1 u_{xt} + Y_1] |_{x_l^+}, \quad (18)$$

where

$$\begin{aligned} S_0 &= \left[\frac{1}{3}(h_0 + \eta)^2 \right] |_{x_l^-}, \\ Y_0 &= \left[\frac{1}{3}(h_0 + \eta)^2(u_x^2 - uu_{xx}) + \frac{1}{2}(u^2 + \frac{1}{3}w^2 + 2g\psi) \right] |_{x_l^-}, \\ R_1 &= -m\eta_x |_{x_l^+}, \\ S_1 &= \left[m(h_1 + \eta) + \frac{1}{3}(h_1 + \eta)^2 \right] |_{x_l^+}, \\ Y_1 &= \left\{ \frac{1}{3}(h_1 + \eta)^2(u_x^2 - uu_{xx}) + \frac{1}{2}(u^2 + \frac{1}{3}w^2 + 2g\psi) + D\eta_{xxx} \right. \\ &\quad \left. + m[(h_1 + \eta)(uu_{xx} + u_x^2) + \eta_{xx}u^2 + 3\eta_x uu_x] \right\} |_{x_l^+} - \phi_t |_{x_l^+} \frac{\rho}{3} [[w]]. \end{aligned} \quad (19)$$

The above two jump conditions correspond to mass and mechanical energy conservation, respectively. The jump conditions can readily be obtained with a similar procedure at the other end of the beam.

B. Linear theory

The linear equations may be obtained readily from the nonlinear theory by expanding each term and ignoring higher-order terms such as $O(u^2)$, $O(u\eta)$, $O(\eta^2)$, etc. In Secs. II B 1 and II B 2, we present the linearized governing equations, initial and boundary conditions and jump conditions. For a formal derivation of the linear GN equations, see, e.g., Ertekin.⁴⁰

1. Governing equations and initial and boundary conditions

After linearizing the nonlinear governing equations, Eqs. (5) and (7), the linear governing equations is obtained as

$$\eta_t + h_1 u_x = 0, \quad (20)$$

$$u_t - \left(\frac{1}{3} h_1^2 + m h_1 \right) u_{xxt} = -\eta_x - D \eta_{xxxxx}. \quad (21)$$

The linearized (integrated) pressure through depth in two-dimensional form is written as

$$\begin{aligned} P &= \frac{1}{3} h_1^2 \eta_{tt} + \frac{1}{2} h_1 (h_1 + 2\eta) + \hat{p}(h_1 + \eta) \\ &= -\frac{1}{3} (h_1^3 + m h_1^2) u_{xt} + \frac{1}{2} h_1^2 + h_0 \eta + h_1 D \eta_{xxxx}. \end{aligned} \quad (22)$$

For the 2D linear problem, we only study the sinusoidal wave case. The fluid layer is quiescent at $t = 0$ and the initial values for all variables are set to zero. The piston wave maker generates the sinusoidal waves at the upwave boundary according to the analytical solutions of the linear GN equations. The sinusoidal motion of the wave-maker is specified as

$$\eta_0(t) = A \cos\left(\frac{\pi}{2} + \omega t\right), \quad u_0(t) = \frac{A\omega}{k} \eta_0(t), \quad (23)$$

where A is the wave amplitude, ω is the angular wave frequency related to the wave period T as $\omega = 2\pi/T$, and k is the wave number of the free surface water wave. The wave number is related to wave frequency for the GN theory through the dispersion relation as discussed later.

The Orlandi open boundary condition is the same as for the three-dimensional nonlinear theory.

At the beam ends, the free-free end boundary conditions at the ends of the beam are the same as in the nonlinear theory, Eq. (14), since the linear beam theory is adopted in this work. The beam end conditions coupled with the fluid may be obtained through the linearization of Eqs. (15) and (16), i.e.,

$$D h_1 u_{xxxxt} = 0, \quad D h_1 u_{xxxxt} = 0. \quad (24)$$

2. Jump conditions

Jump conditions for the linear theory are simplified from the nonlinear derivation by ignoring the higher-order terms in Eqs. (17)–(19). The jump conditions for the mass and energy conservations at the left end of the beam are

$$hu \Big|_{x_i^-} = hu \Big|_{x_i^+}, \quad (25)$$

$$\left[-\frac{1}{3} \rho h_0^2 u_{xt} + \rho g \eta \right] \Big|_{x_i^-} = \left[-\frac{1}{3} \rho h_1^2 u_{xt} + \rho g \eta - m h_1 u_{xt} + D \eta_{xxxx} \right] \Big|_{x_i^+}. \quad (26)$$

The jump conditions at the other end of the beam can similarly be obtained.

3. Linear dispersion relations for water wave and hydroelastic wave

The dispersion relation for the linear GN theory is given by Green *et al.*⁴¹ Its dimensional form is

$$k^2 = \frac{3\omega^2}{3gh - h^2\omega^2} \text{ or } \omega^2 = \frac{3ghk^2}{3 + h^2k^2}, \quad (27)$$

where k is the wave number and ω is the angular wave frequency. Compared with the dispersion relation of the linear potential theory, i.e., $\omega^2 = gk \tanh(kh)$, the error in estimation of ω by the GN theory is $O(k^6 h^6)$.

The celerity, c and group velocity, c_g for the GN theory can be derived from Eq. (27):

$$c = \frac{\omega}{k} = \sqrt{\frac{3gh}{3 + h^2k^2}}, \quad c_g = \frac{d\omega}{dk} = \frac{3c}{3 + h^2k^2}. \quad (28)$$

Compared with the celerity of the exact potential theory, i.e., $c = \sqrt{g \tanh(kh)/k}$, Kim and Ertekin⁴² showed that the relative error of the GN celerity is within 1% when $kh < 1$ and 6% when $kh < 2$.

Kim and Ertekin⁴² derived the celerity, c_p , and group velocity, c_{pg} of the hydroelastic waves for the linear GN theory:

$$c_p = \frac{\omega}{k_p} = \sqrt{\frac{Dk_p^4 + \rho g}{\rho/h_1 + (m + \rho h_1/3)k_p^2}}, \quad (29)$$

$$c_{pg} = \frac{d\omega}{dk_p} = \frac{3\rho^2 g + Dk_p^4(6mk_p^2 h_1 + 9\rho + 2\rho k_p^2 h_1^2)}{3h_1(Dk_p^4 + \rho g)[\rho/h_1 + (m + \rho h_1/3)k_p^2]}.$$

The exact dispersion relation based on the linear exact potential and thin plate theories are given in Davys *et al.*:⁴³

$$c_p = \frac{\omega}{k_p} = \sqrt{\frac{Dk_p^4 + \rho g}{\{m + \rho/[k_p \tanh(k_p h_1)]\}k_p^2}}. \quad (30)$$

The agreement between the dispersion relations for the hydroelastic wave by the GN theory and the exact linear potential theory is better than that for the free surface water waves, since there is no approximation of the bending term, Dk_p^4 , in the GN theory.

III. NUMERICAL SCHEME

The numerical method used to solve the problem is the same as used by Xia *et al.*²⁹ The Runge-Kutta method of order four was used to march in time. The second-order accurate central-difference formulas are used for the spatial derivatives. The mass continuity equation can be solved in a straight forward manner. In the momentum equation, the time derivatives involve the spatial derivatives, e.g., u_{xt} and u_{xxt} , which cannot be solved explicitly. These can be solved through a simultaneous set of linear equations in two steps. To use the central difference method for the derivatives of u at x_1^\pm , fictitious points are introduced on each side, as depicted in Fig. 2.

To monitor the numerical accuracy of the predictions, both the mass and energy conservation were monitored in time. For the mass conservation (see, e.g., Chian and Ertekin⁴⁴), the total mass change in a region bounded by upwave boundary $x = x_U$, and downwave boundary $x = x_D$ at a specific time t is

$$\Delta M_w(t) = M_w(t) - \Delta M_{wU}(t) + \Delta M_{wD}(t) - M_w(0), \quad (31)$$

where the total mass at time t in the target region is $M_w(t) = \int_{x_U}^{x_D} (1 + \eta) dx$, the total mass flow through the upwave boundary and downwave boundary from the beginning of calculation ($t = 0$) to time t are, respectively, $\Delta M_{wU}(t) = \int_0^t (1 + \eta) u|_{x_U} dt$ and $\Delta M_{wD}(t) = \int_0^t (1 + \eta) u|_{x_D} dt$, and $M_w(0)$

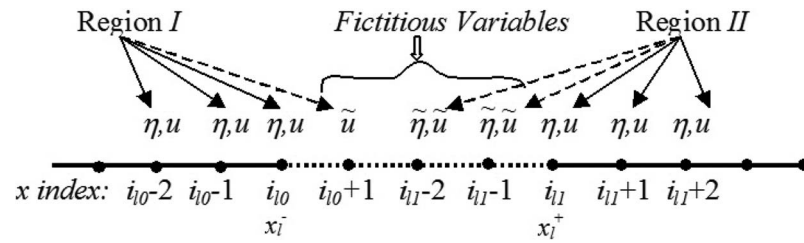


FIG. 2. Fictitious points introduced to use the central difference formulas.

is the initial total mass in the region monitored. The percent change in mass due to numerical errors can be calculated through

$$\Delta M_{wE}(t) = \frac{\Delta M_w(t)}{M_w(0)} \times 100\%. \quad (32)$$

The energy conservation is monitored similarly as that for the mass conservation. The relative errors for both energy and mass conservation are found to be less than 5% for all the cases considered here.

To make the numerical scheme stable, the unwanted saw-tooth-oscillations of high wave frequency were removed by use of a five-point filtering formula that Ertekin⁴⁰ and Demirbilek and Webster⁴⁵ used successfully.

IV. RESULTS AND DISCUSSION

We first verify the linear model that we developed based on the linearized GN equations as well as Kirchoff theory. This is followed by the analysis of the nonlinear response of the runway to cnoidal waves. The nonlinear results are also compared with the linear results to better understand the importance of nonlinearity. We also study the effect of beam stiffness on the hydroelastic response. To do this, the same runway considered by Kashiwagi¹² and Ertekin and Kim¹⁴ is further studied for both wave conditions, and for the flexural rigidity of $D/\rho gh_0^4 = 3.2$, length of the beam $B/h_0 = 20$, and draft $d/h_0 = 0.1$. The main dimensions used in the problem are listed in Table I. Note that, in this two-dimensional problem, B is the length for us as the waves impinge on the runway as beam waves.

A. Verification of the linear model

The verification of the linear theory is carried out by comparing the current GN results obtained through time domain analysis with those from frequency domain analysis of the linear GN equations obtained by Kim and Ertekin⁴² and the experimental data of Wu *et al.*⁶ The physical properties and dimensions of the plate used are given as $D = 471$ Nm, $L = 10$ m, $d = 0.00836$ m, and $h_0 = 1.1$ m. The wave number of the incoming wave is $kh = 2.03$, which corresponds to a wave period of 1.43 s.

TABLE I. Parameters of A mat-type floating runway.

Parameter	Dimensional value	Nondimensional
Length, L	5000 m	100
Width, B	1000 m	20
Draft, d	5 m	0.1
Displacement	25 000 000 mT	200
Flexural rigidity, $D = EI/B$	1.96×10^{11} Nm	3.2
Poisson's ratio, ν	...	0.3
Water depth, h_0	50 m	1
ρ_w	1000 kg/m ³	1
g	9.8 m/s ²	1

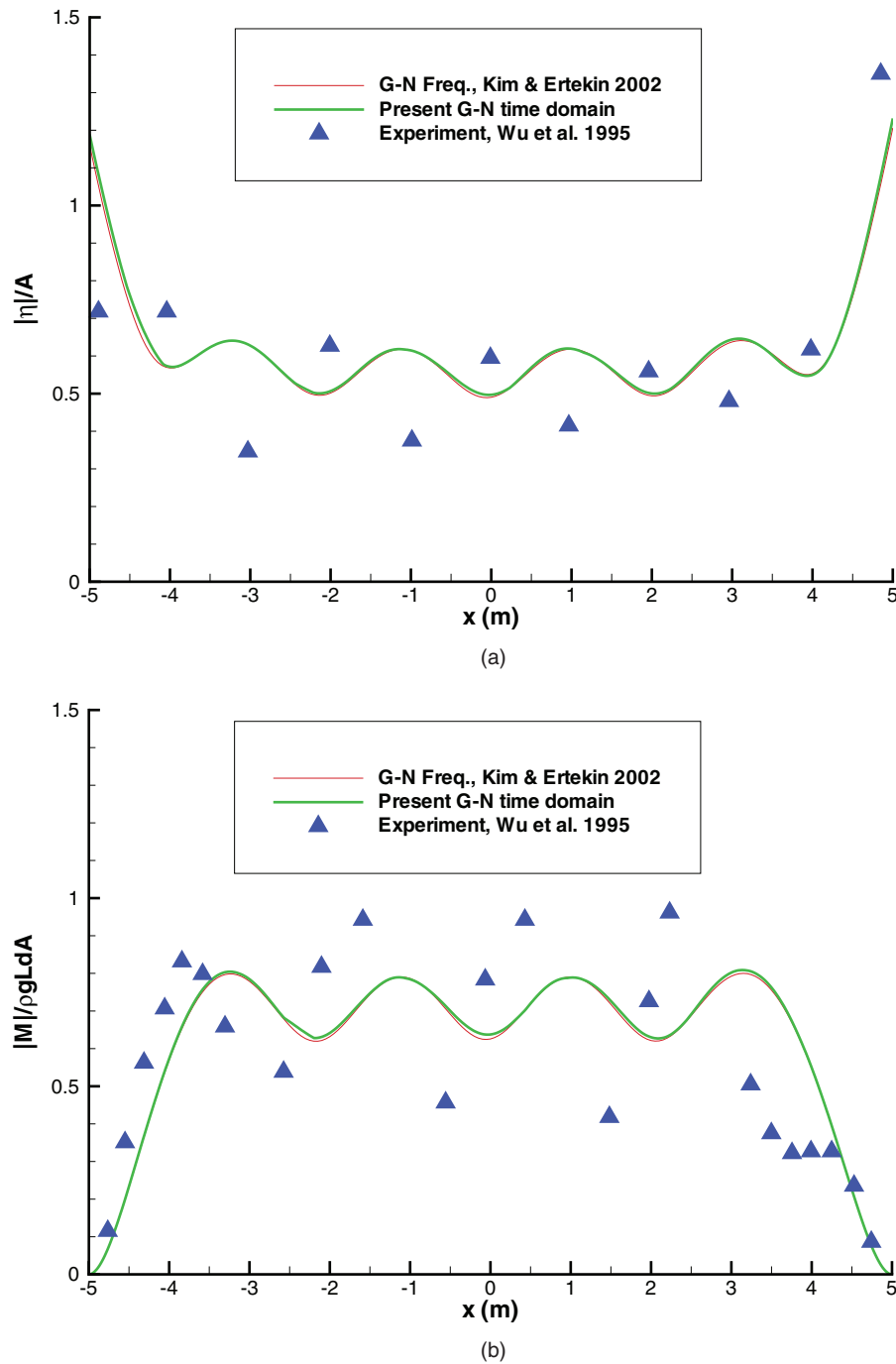


FIG. 3. Comparison of the (a) displacement amplitude and (b) bending moment amplitude based on the linear GN theory with other results: $kh = 2.03$.

In Fig. 3, the amplitudes of vertical displacement and bending moment are compared with the experimental data of Wu *et al.*⁶ and the analytical results of Kim and Ertekin.⁴² The results show that the GN results from the current time-domain analysis and the analytical frequency domain are almost identical. The comparison between the GN results and experimental data shows that the trend in both the maximum displacement and bending moment agrees well in general. However, there are some discrepancies in the peak values.

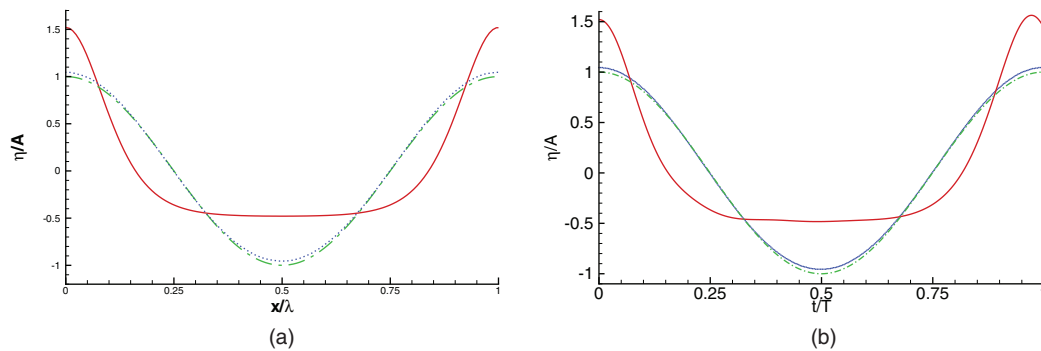


FIG. 4. Comparison of linear and nonlinear incoming waves for $\lambda/h_0 = 25.13$. (a) Surface elevation profiles vs. length and (b) surface profile time history: cnoidal wave $A/h_0 = 0.075$ —; cnoidal wave $A/h_0 = 0.002$ ---; and linear sinusoidal wave $A/h_0 = 0.075$ - · -.

B. Cnoidal waves

The nonlinear hydroelastic response to cnoidal waves is first compared with the linear response to a sinusoidal wave. Note that for any given wave period, it is not possible to match the wave lengths for the two wave types. This is because the period of a cnoidal wave depends on both the wave length and amplitude, while the wave period of a linear sinusoidal wave is only dependent on the wave length. However, for a given wave length, the period of a cnoidal wave converges to the value for the linear sinusoidal wave when the amplitude of the cnoidal wave tends to become infinitesimally small. In the comparison, the same wave length is used for both the linear and nonlinear waves.

The wave length studied is $\lambda/h_0 = 25.13$. For the linear sinusoidal wave, the corresponding wave period and wave number are $T/\sqrt{h_0/g} = 25.4$ and $kh_0 = 0.25$, respectively. Two wave amplitudes are considered for the cnoidal wave, i.e., $A/h_0 = 0.075$ and 0.002 . Based on the nonlinear dispersion relation, Eq. (13), the nondimensional wave periods for both cnoidal waves are $T_{CN}/(h_0/g)^{0.5} = 24.7$ and 25.4 , respectively. The profile and time history of the surface elevations for these wave conditions are shown in Fig. 4. In these plots, the x and t axes are normalized by wave length λ and linear wave period T , respectively. The surface profiles for the linear sinusoidal wave and cnoidal wave with very small amplitude are almost identical, and they are symmetric about the still-water surface. However, for the larger amplitude cnoidal wave, the wave crest and trough are not symmetric about the still-water surface and the crest is much higher than that for the linear wave.

The time histories of the hydroelastic deformation and wave run-up at the ends of the beam for the wave conditions discussed above, are shown in Figs. 5 and 6, respectively. The run-up is given by the difference between the wave elevation and structural deformation at the interface of Regions I and II. The maximum displacement and bending moment along the structure are shown in Fig. 7.

It is shown that the time histories of dynamic response are fully developed during the last two wave cycles. The nonlinear response converges to the linear one when the wave amplitude is very small. The nonlinear hydroelastic response to a cnoidal wave with large-amplitude is larger than the linear response, especially for the wave run-up and maximum bending moment. This is due to the high nonlinearity of the large amplitude cnoidal wave which is apparent from the uneven distribution of crest and trough, and the higher harmonics as can be seen in the response time histories.

The effect of the cnoidal wave amplitude on hydroelastic response is further studied. The maximum response of displacement and bending moment along the structure are shown in Fig. 8. The wave length for these cases is $\lambda/h_0 = 25.13$, and the wave amplitudes are $A/h_0 = 0.001, 0.005, 0.05,$ and 0.1 , respectively. The results show that normalized bending moment increases with the increase of wave amplitude and the displacements at the beam ends are also significantly affected by the wave amplitudes.

The hydroelastic response to different stiffnesses is also studied, similar to the solitary wave case studied by Xia *et al.*²⁹ The maximum responses for a cnoidal wave amplitude of $A/h_0 = 0.05$ and wave length $\lambda/h_0 = 25.13$ are shown in Fig. 9. The linear response for a sinusoidal wave with the same wave length is shown in Fig. 10 for comparison purposes.

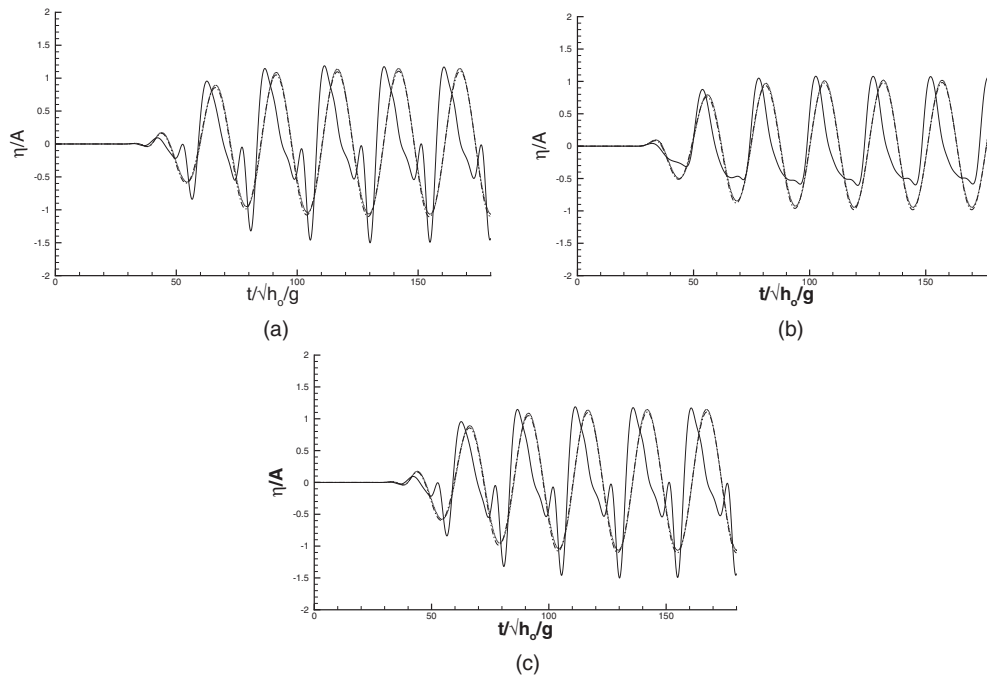


FIG. 5. Comparison of linear and nonlinear responses for $\lambda/h_0 = 25.13$ — displacement time history: cnoidal wave $A/h_0 = 0.075$ —; cnoidal wave $A/h_0 = 0.002$ ···; and linear sinusoidal wave $A/h_0 = 0.075$ - - -. (a) Upwave beam end, (b) middle point of beam, and (c) downwave beam end.

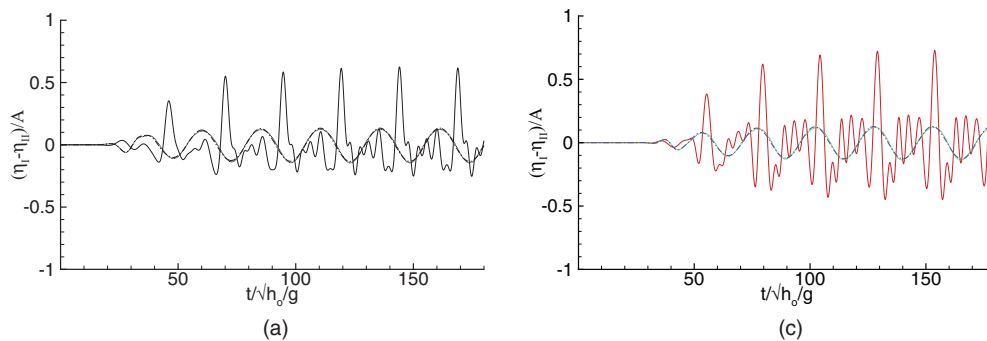


FIG. 6. Comparison of linear and nonlinear responses for $\lambda/h_0 = 25.13$ - wave runup time history: Cnoidal wave $A/h_0 = 0.075$ —; Cnoidal wave $A/h_0 = 0.002$ ···; Linear sinusoidal wave $A/h_0 = 0.075$ - - -. (a) Upwave beam end and (b) downwave beam end.

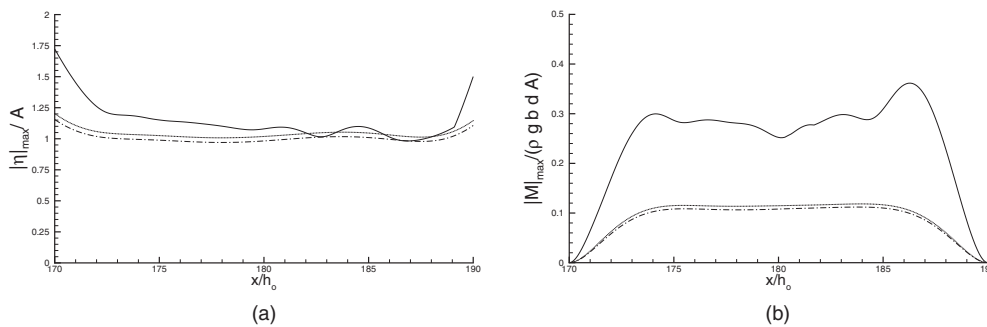


FIG. 7. Comparison of linear and nonlinear responses for $\lambda/h_0 = 25.13/h_0$ — (a) maximum displacement and (b) maximum bending moment on the structure: cnoidal wave $A/h_0 = 0.075$ —; cnoidal wave $A/h_0 = 0.002$ ···; and linear sinusoidal wave $A/h_0 = 0.075$ - - -.

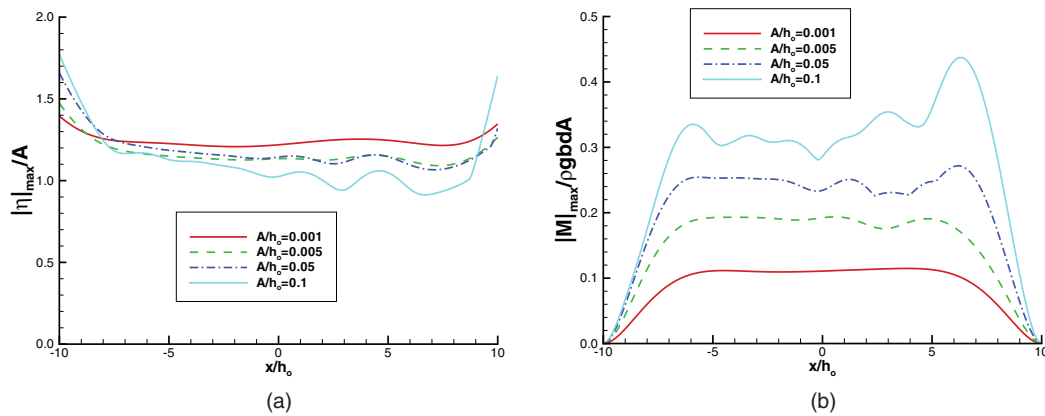


FIG. 8. Maximum responses along the VLFS for various cnoidal wave amplitudes ($\lambda/h_0 = 25.13$, $D/\rho g h_0 = 3.2$): (a) maximum displacement and (b) maximum bending moment.

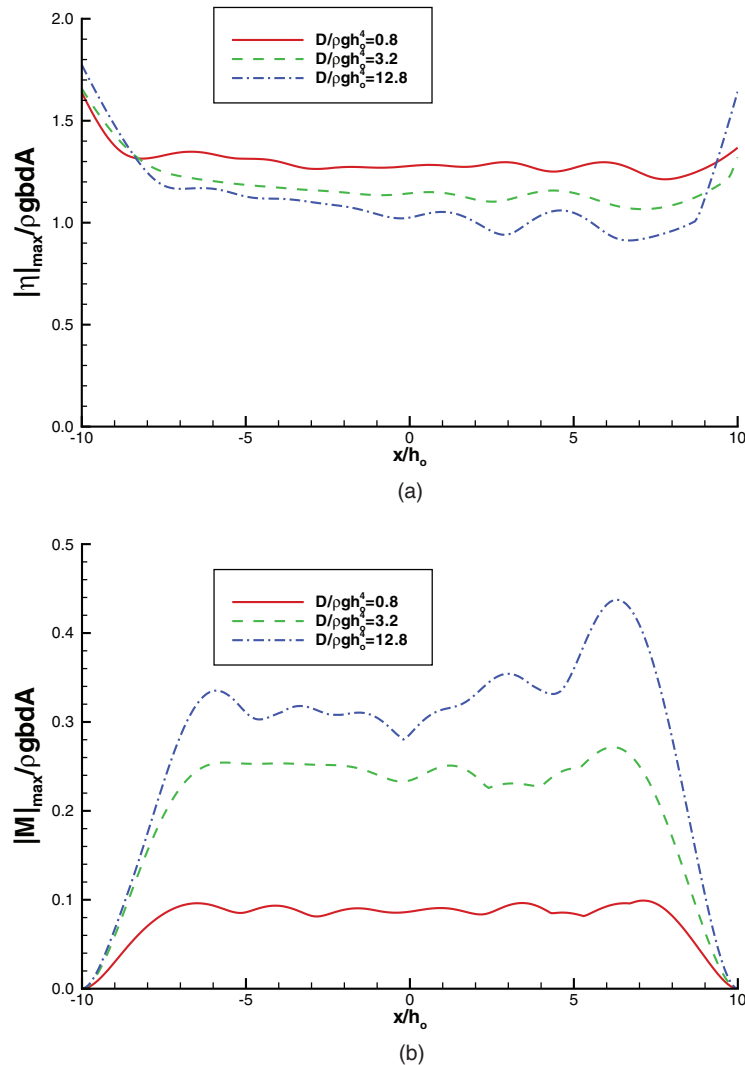


FIG. 9. Maximum responses along the VLFS for various stiffnesses based on nonlinear theory ($\lambda/h_0 = 25.13$, $A/h_0 = 0.05$): (a) maximum displacement and (b) maximum bending moment.

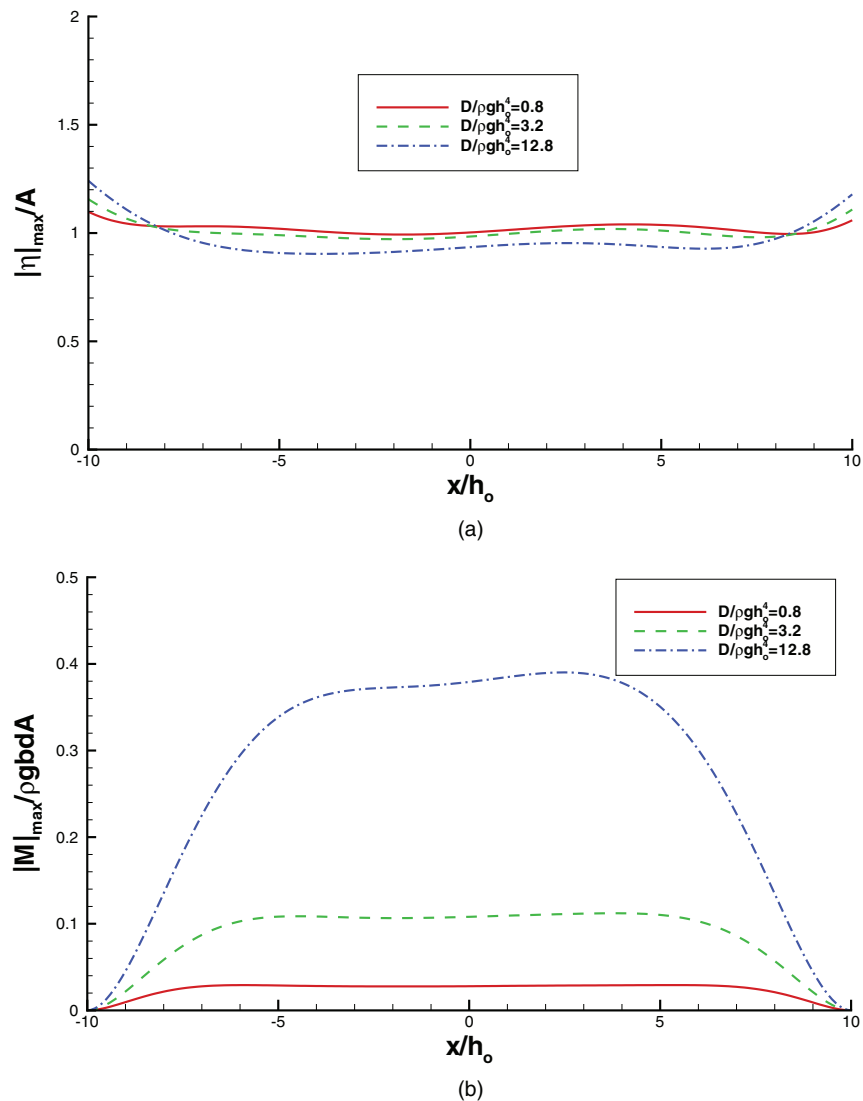


FIG. 10. Maximum responses along the VLFS for various stiffnesses based on linear theory ($\lambda/h_0 = 25.13$): (a) maximum displacement and (b) maximum bending moment.

The nonlinear response is higher than the linear response for both the displacement and bending moment. The bending moment increases with the increase of bending stiffness. However, the linear bending moment response is almost proportional to bending stiffness while the nonlinear response is not. The differences between the bending moments for higher stiffnesses are much smaller than that for lower stiffnesses.

V. CONCLUSIONS

A modified set of Level I GN equations that represent a long wave beneath an elastic plate in two dimensions have been used. Jump conditions are enforced in the solution of the governing equations. The solutions of the ordinary GN equations in the open water region and that of the modified GN equations under the structure are obtained by the finite-difference method. Numerical results showing the behavior of cnoidal waves beneath an elastic plate are presented and compared with the linear GN predictions.

The linear model is verified by comparing the present linear numerical results in the time-domain with the experimental data and the linear GN results in the frequency domain for a sinusoidal incoming wave. The present time-domain GN results are almost identical to the GN frequency-domain results. The nonlinear response for a cnoidal wave converge to the linear solution for a sinusoidal wave with the same wave length as the cnoidal wave, when the cnoidal wave height is very small. However, as the wave height increases, the nonlinear responses on displacement and bending moment are much higher than the linear solutions. This is due to the uneven distribution of the crest and trough of the cnoidal wave and higher harmonics present in the cnoidal wave. It is also shown that the nonlinearity is important in predicting wave run-up. Similar results were obtained before when tsunami impacts a floating runway, see Xia *et al.*²⁹

It is known that the Green-Naghdi theory with more directors, i.e., higher Level of approximation, can predict the dispersion relation more accurately for short waves than the Level I GN theory can. It is recommended therefore that a higher-level GN theory be used to study the hydroelasticity of VLFS in all water depths in the future, see, e.g., Demirbilek and Webster,⁴⁵ Shields and Webster,⁴⁶ and Zhao *et al.*⁴⁷ The structural model can also be improved by adopting a more accurate linear theory, e.g., Mindlin plate theory as suggested by Wang *et al.*,⁹ or a nonlinear theory such as the Green-Naghdi plate theory (see, e.g., Naghdi⁴⁸).

ACKNOWLEDGMENTS

This research is based partially upon work supported by ONR Grant No. N000149-81-0800, NSF Grant No. BES-9532037, and ONR Grant No. N000140-21-0903.

- ¹ *Proceedings of the First International Workshop on Very Large Floating Structures, VLFS '91*, (TC1665 .1596), edited by R.C.Ertekin and H. R. Riggs (University of Hawaii, Honolulu, Hawaii, 1991).
- ² E. Watanabe, T. Utsunomiya, and C. M. Wang, "Hydroelastic analysis of pontoon-type VLFS: A literature survey," *Eng. Struct.* **26**, 245–256 (2004).
- ³ M. Kashiwagi, "Research on hydroelastic responses of VLFS: Recent progress and future work," *Int. J. Offshore Polar Eng.* **10**(2), 81–90 (2000).
- ⁴ S. Ohmatsu, "Overview: Research on wave loading and responses of VLFS," *Mar. Struct.* **18**, 149–168 (2005).
- ⁵ Y. S. Wu, "Hydroelasticity of floating bodies," Ph.D. thesis (Brunel University, UK, 1984), v+263pp.
- ⁶ C. Wu, E. Watanabe, and T. Utsunomiya, "An eigenfunction expansion-matching method for analyzing the wave-induced responses of an elastic floating plate," *Appl. Ocean Res.* **17**, 301–310 (1995).
- ⁷ S. Nagata, Y. Yoshida, T. Fujita, and H. Isshiki, "The analysis of wave-induced response of an elastic floating plate in a sea with a breakwater," in *Proceedings of the 8th International Offshore and Polar Engineering, Montréal, Canada* (International Society of Offshore and Polar Engineers, Mountain View, CA, 1998), pp. 223–230.
- ⁸ M. Kashiwagi, "A B-spline Galerkin method for computing hydroelastic behaviors of a very large floating structure," in *Proceedings of the International Workshop on Very Large Floating Structures, Hayama, Japan* (Ship Research Institute, Tokyo, Japan, 1996), pp. 149–156.
- ⁹ C. M. Wang, Y. Xiang, T. Utsunomiya, and E. Watanabe, "Evaluation of modal stress resultants in freely vibrating plates," *Int. J. Solids Struct.* **38**(36–37), 6525–6558 (2001).
- ¹⁰ P. Mamidipudi and W. C. Webster, "The motions performance of a mat-like floating airport," in *First International Conference on Hydroelasticity in Marine Technology (Hydroelasticity '94)*, edited by O. M. Faltinsen, C. M. Larsen, T. Moan, K. Holden, and N. Spidsoe (A.A. Balkema, Rotterdam/Trondheim/ Norway, 1994), pp. 363–375.
- ¹¹ J. Ma, "Structural optimization of large-scale floating runways using a floating-mat hydrodynamic model," Ph.D. thesis (U.C. Berkeley, 2003), vi+325pp.
- ¹² M. Kashiwagi, "A B-spline Galerkin scheme for calculating the hydroelastic response of a very large floating structure in waves," *J. Mar. Sci. Tech.* **3**(1), 37–49 (1998).
- ¹³ M. Ohkusu, and Y. Namba, "Analysis of hydroelastic behavior of a large floating platform of thin plate configuration in waves," in *Proceedings of the International Workshop on Very Large Floating Structures, VLFS '96, Hayama, Japan*, edited by Y. Watanabe (Ship Research Institute, Tokyo, Japan, 1996), pp. 143–148.
- ¹⁴ R. C. Ertekin and J. W. Kim, "Hydroelastic response of a mat-type structure in oblique, shallow-water wave," *J. Ship Res.* **43**, 241–254 (1999).
- ¹⁵ H. R. Riggs, H. Suzuki, R. C. Ertekin, J. W. Kim, and K. Iijima, "Comparison of hydroelastic computer codes based on the ISSC VLFS benchmark," *Ocean Eng.* **35**, 589–597 (2008).
- ¹⁶ HYDRAN, "A computer program for the hydroelastic response analysis of ocean structures," Technical Report (Offcoast Inc., Kailua, HI, 2012).
- ¹⁷ K. Iijima, K. Yoshida, and H. Suzuki, "Hydrodynamic and hydroelastic analyses of very large floating structures in waves," in *Proceedings of the 16th International Conference on Offshore Mechanics and Arctic Engineering (OMAE '97), Yokohama, Japan* (American Society of Mechanical Engineers, New York, 1997), pp. 139–145.

- ¹⁸ D. Xia, J. W. Kim, and R. C. Ertekin, "The effect of shoreline proximity on the hydroelastic response of a floating runway," in *Proceedings of the 18th International Conference on Offshore Mechanics and Arctic Engineering (OMAE '99)*, St. John's, Newfoundland, Canada (American Society of Mechanical Engineers, New York, 1999), pp. 8.
- ¹⁹ R. C. Ertekin, J. W. Kim, and D. Xia, "Hydroelastic response of a mat-type, floating runway near a breakwater in irregular seas," in *Proceedings of the Oceans'99 Conference, Seattle, Washington (MTS/IEEE, Washington, D.C., 1999)*, pp. 9.
- ²⁰ S. Ohmatsu, "Numerical calculation of hydroelastic behaviour of VLFS in time domain," in *Proceedings of the 2nd International Conference on Hydroelasticity in Marine Technology*, edited by M. Kashiwagi, W. Koterayama, and M. Ohkusu (Yomei Printing Cooperative Society, RIAM, Kyushu University, Fukuoka, Japan, 1998), pp. 89–97.
- ²¹ Q. Miao, S. Du, S. Dong, and Y. Wu, "Hydrodynamic analysis of a moored very large floating structure," in *Proceedings of the International Workshop on Very Large Floating Structures, VLFS'96, Hayama, Japan*, edited by Y. Watanabe (Ship Research Institute, Tokyo, Japan, 1996), pp. 201–208.
- ²² O. M. Faltinsen, "Bottom slamming on a floating airport," in *Proceedings of the International Workshop on Very Large Floating Structures, (VLFS'96)* (Ship Research Institute, Tokyo, Japan, 1996), pp. 97–106.
- ²³ J. W. Kim and R. C. Ertekin, "An eigenfunction expansion method for predicting hydroelastic behavior of a shallow draft VLFS," in *Proceedings of the 2nd International Conference on Hydroelasticity in Marine Technology*, edited by M. Kashiwagi, W. Koterayama, and M. Ohkusu (Yomei Printing Cooperative Society, Fukuoka, Japan, 1998), pp. 47–59.
- ²⁴ M. Kashiwagi, "A B-spline Glerkin scheme for computing wave forces on a floating very large elastic plate," in *Proceedings of the 7th International Offshore and Polar Engineering Conference, Honolulu, Hawaii* (International Society Offshore and Polar Engineers, Mountain View, CA, 1997), pp. 229–236.
- ²⁵ X. Liu and S. Sakai, "Time domain analysis on the dynamic response of a flexible floating structure to waves," *J. Eng. Mech.* **128**(1), 48–56 (2002).
- ²⁶ K. Takagi, "Interaction between solitary wave and floating elastic plate," *J. Waterway, Port, Coastal, Ocean Eng.* **123**, 57–62 (1997).
- ²⁷ K. Takagi, "Interaction between tsunami and artificial floating island," *Int. J. Offshore Polar Eng.* **6**, 171–176 (1996).
- ²⁸ T. Y. Wu, "Long waves on ocean and coastal waters," *J. Eng. Mech.* **107**, 501–522 (1981).
- ²⁹ D. Xia, R. C. Ertekin, and J. W. Kim, "Fluid-structure interaction between a two-dimensional mat-type VLFS and solitary waves by the Green-Naghdi theory," *J. Fluids Struct.* **24**, 527–540 (2008).
- ³⁰ A. E. Green and P. M. Naghdi, "A derivation of equations for waves propagation in water of variable depth," *J. Fluid Mech.* **78**, 237–246 (1976).
- ³¹ S. P. Timoshenko and S. Woinowsky-Krieger, *Theory of Plates and Shells* (McGraw-Hill, New York, 1959).
- ³² R. C. Ertekin, W. C. Webster, and J. V. Wehausen, "Waves caused by a moving disturbance in a shallow channel of finite width," *J. Fluid Mech.* **169**, 275–292 (1986).
- ³³ R. C. Ertekin and J. V. Wehausen, "Some soliton calculations," in *Proceedings of the 16th Symposium on Naval Hydrodynamics, Berkeley* (National Academy Press, Washington, D.C., 1987, 1986), pp. 167–185.
- ³⁴ R. C. Ertekin and J. M. Becker, "Nonlinear diffraction of waves by a submerged shelf in shallow water," *J. Offshore Mech. Arctic Eng.* **120**, 212–220 (1998).
- ³⁵ R. C. Ertekin, "Nonlinear shallow-water waves: The Green-Naghdi equations," in *Proceedings of Pacific Congress on Marine Science and Technology* (PACON, Honolulu, Hawaii, 1988), pp. OST6/42–OST6/52.
- ³⁶ D. Xia, "Linear and nonlinear hydroelasticity of mat-type very large floating structures: The Green-Naghdi theory," Ph.D. thesis (University of Hawaii, 2006), xiv+145pp.
- ³⁷ X. F. Sun, "Some theoretical and numerical studies on two-dimensional Cnoidal-wave diffraction problems," Master's thesis (University of Hawaii at Manoa, 1991), xii+149pp.
- ³⁸ P. M. Naghdi and M. B. Rubin, "On the transition to planing of a boat," *J. Fluid Mech.* **103**, 345–374 (1981).
- ³⁹ A. E. Green and P. M. Naghdi, "A nonlinear theory of water waves for finite and infinite depths," *Philos. Trans. R. Soc. London, Ser. A* **320**, 37–70 (1986).
- ⁴⁰ R. C. Ertekin, "Soliton generation by moving disturbances in shallow water: Theory, computation and experiment," Ph.D. thesis (U.C. Berkeley, 1984), v+352pp.
- ⁴¹ A. E. Green, N. Laws, and P. M. Naghdi, "On the theory of water waves," *Proc. R. Soc. London, Ser. A* **338**, 43–55 (1974).
- ⁴² J. W. Kim and R. C. Ertekin, "Hydroelasticity of an infinitely long plate in oblique waves: linear Green-Naghdi theory," *J. Eng. Maritime Environ.* **216**, 179–197 (2002).
- ⁴³ J. W. Davys, R. H. Hosking, and A. D. Sneyd, "Waves due to a steadily moving source on a floating ice plate," *J. Fluid Mech.* **158**, 269–287 (1985).
- ⁴⁴ C. Chian and R. C. Ertekin, "Diffraction of solitary waves by submerged horizontal cylinders," *Wave Motion* **15**, 121–142 (1992).
- ⁴⁵ Z. Demirbilek and W. C. Webster, "Application of the Green-Naghdi theory of fluid sheets to shallow-water wave problems," Technical Report CERC-92-11 (U.S. Army Corps of Engineers, Waterways Experiment Station, Vicksburg, MS, 1992).
- ⁴⁶ J. S. Shields and W. C. Webster, "On direct methods in water-wave theory," *J. Fluid Mech.* **197**, 171–199 (1988).
- ⁴⁷ B. Zhao, W. Y. Duan, and R. C. Ertekin, "Application of higher-level GN theory to some wave transformation problems," *Coastal Eng.* **83**, 177–189 (2014).
- ⁴⁸ P. M. Naghdi, "Mechanics of Solids II in Encyclopedia of Physics," in *The Theory of Shells and Plates* (Springer-Verlag, Berlin, Germany, 1972), pp. 425–640.